



A simple route for the synthesis of 3,3,3',3'-tetramethyl-2,3,3',4'-tetrahydro-1*H*,1'*H*-[4,9'-bixanthene]-1,1'(2'*H*,9'*H*)-dione and its derivatives catalyzed by Mn²⁺ and other transition metal cations

Nader Noroozi Pesyan^{a,*}, Vali Golsanamloo^a, Shahnaz Ganbari^a, Ertan Şahin^b

^a Department of Chemistry, Faculty of Science, Urmia University, 57159 Urmia, Iran

^b Department of Chemistry, Faculty of Science, Atatürk University, 25240 Erzurum, Turkey

ARTICLE INFO

Article history:

Received 21 February 2012

Revised 5 May 2012

Accepted 24 May 2012

Available online 30 May 2012

Keywords:

Coupling reaction

Metal cation

Dimedone

[4,9'-Bixanthene]-1,1'(2'*H*,9'*H*)-dione

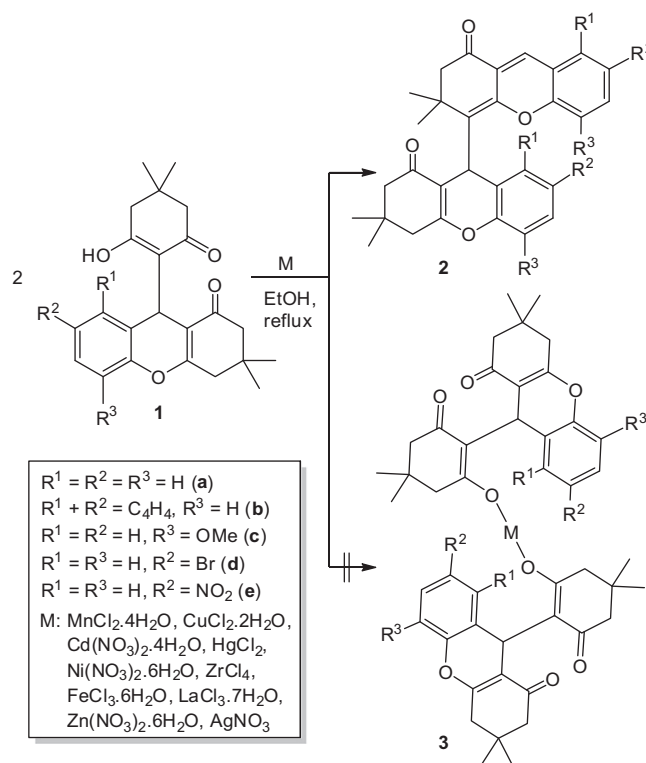
ABSTRACT

A simple and efficient unusual coupling reaction of 9-(2-hydroxy-4,4-dimethyl-6-oxocyclohex-1-en-1-yl)-3,3-dimethyl-2,3,4,9-tetrahydro-1*H*-xanthen-1-one and its derivatives was accomplished in the presence of Mn²⁺, Cu²⁺, Cd²⁺, Hg²⁺, Fe³⁺, or La³⁺. The structure elucidation was accomplished by IR, ¹H NMR, ¹³C NMR, X-ray crystallography, UV–Visible and elemental analysis. A reaction mechanism is proposed.

Crown Copyright © 2012 Published by Elsevier Ltd. All rights reserved.

Organic molecules containing xanthene moieties are of biological importance and are useful in drug discovery.¹ The xanthene derivative, (9*S*)-9-(2-hydroxy-4,4-dimethyl-6-oxocyclohex-1-en-1-yl)-3,3-dimethyl-2,3,4,9-tetrahydro-1*H*-xanthen-1-one is a selective and orally active neuropeptide Y₅ receptor antagonist.^{1b–d} Chromenes are an important class of compounds, and are often found as the main components of many naturally occurring products employed as cosmetics, pigments, and as potential biodegradable agrochemicals.^{1e–i} Some xanthene derivatives demonstrate photo-activated insecticidal and pest-control activity,^{1j,1k} and anticancer properties.^{1l}

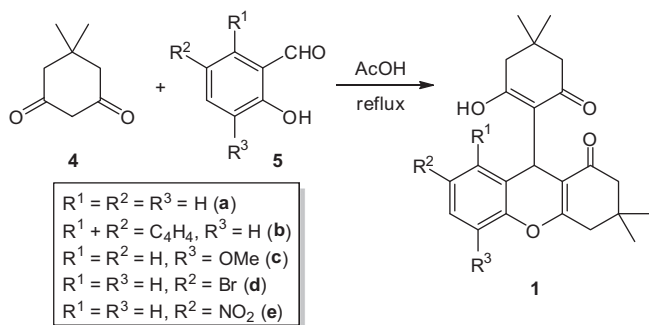
Xanthenes are also very efficient laser dyes and show outstanding photophysical properties.² For example, the aggregation phenomena of xanthene dyes has been reviewed,^{2d} as has their photochemistry,^{2e} electron transfer,^{2f} triplet absorption spectra,^{2g} and photodegradation.^{2h} For the fluoresceins in particular, the photochemistry of rhodamines has been investigated^{2j} as has hydrogen generation during the photolysis of water.^{2k} There have been many new uses for xanthenes reported. These include as nonlinear optical (NLO) materials,^{3a} charge control agents in electrophotographic toners (laser printers and photocopiers),^{3b} and as markers or biological stains.^{3c} Rhodamines and rosamines, in particular, have been used in inks for ink-jet printers. There has also



Scheme 1. Coupling reaction of 1 in the presence of various metal cations giving 2.

* Corresponding author.

E-mail address: n.noroozi@urmia.ac.ir (N. Noroozi Pesyan).



Scheme 2. Reaction of dimedone (**4**) with salicylaldehyde (**5a**) and its derivatives **5b–5e**.

been a significant amount of activity on the use of xanthenes, and in particular rhodamines, as laser dyes.^{3d}

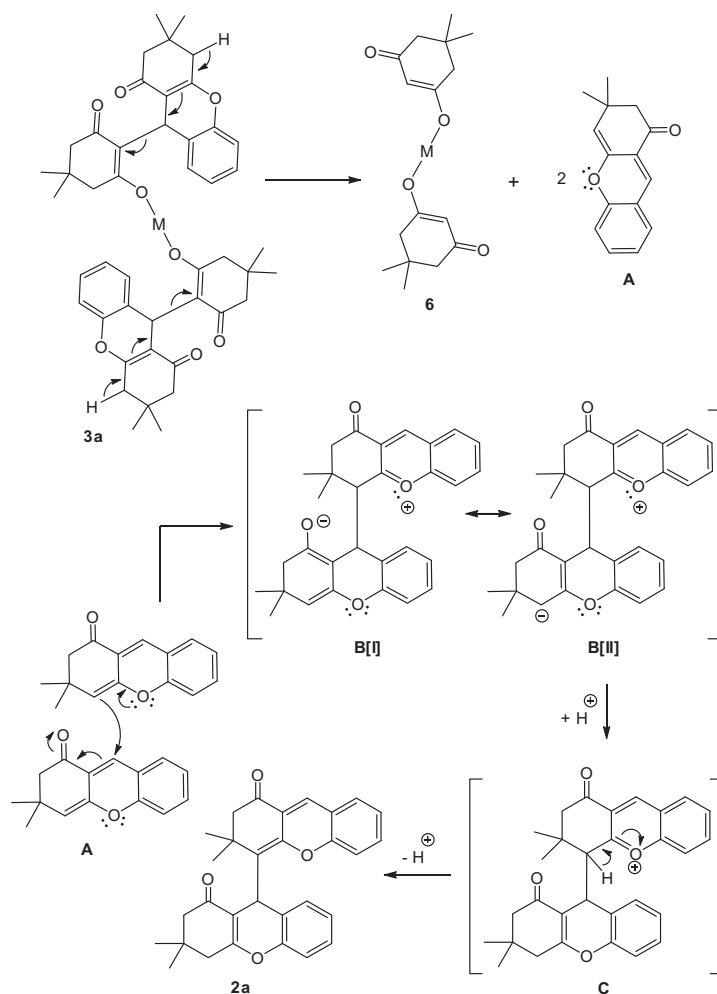
As part of our ongoing studies on the synthesis of dimeric xanthene derivatives, herein we report the unusual coupling of 4-(3,3-dimethyl-1-oxo-2,3,4,9-tetrahydro-1H-xanthen-9-yl)-5-hydroxycyclohex-4-ene-1,3-dione (**1a**) and its derivatives **1b–e** in the presence of various transition metal cations (Scheme 1).⁴

Our initial aim was to attempt the synthesis of a metal complex **3** via the reaction of **1** with transition metal cations originating from $MnCl_2 \cdot 4H_2O$, $CuCl_2 \cdot 2H_2O$, $Cd(NO_3)_2 \cdot 4H_2O$, $HgCl_2$, $Ni(NO_3)_2 \cdot 6H_2O$, $ZrCl_4$, $FeCl_3 \cdot 6H_2O$, $LaCl_3 \cdot 7H_2O$, $Zn(NO_3)_2 \cdot 6H_2O$, or $AgNO_3$.

However, this reaction was unsuccessful in the presence of all these mentioned transition metal cations. The unusual coupling reaction of **1a–e** in the presence of $MnCl_2 \cdot 4H_2O$, $CuCl_2 \cdot 2H_2O$, $Cd(NO_3)_2 \cdot 4H_2O$, $HgCl_2$, $FeCl_3 \cdot 6H_2O$, and $LaCl_3 \cdot 7H_2O$ afforded dimers **2a–e** in good yields (Scheme 1 and Table 1).

In the IR spectrum of **2a**, the hydroxy frequency disappeared in comparison with that of **1a** at 3181 cm^{-1} . The 1H NMR spectrum of **2a** showed three singlets for the four methyl protons at δ 0.95, 1.11, and 1.48, a singlet for the aliphatic C–H proton at δ 4.85 and a multiplet for the diastereotopic methylene protons in the range δ 2.29–2.64. In the aromatic region, a triplet at δ 6.87 (1H), two multiplets at δ 6.94–6.98 (3H) and at δ 7.05–7.10 (3H), and a triplet at δ 7.20 were also shown. The ^{13}C NMR spectrum of **2a** showed thirty distinct peaks. The UV–visible spectrum of **2a** demonstrated absorption maxima at 469 nm in ethanol. These data confirmed the structure of **2a**. We performed these reactions in the presence of $FeCl_3 \cdot 6H_2O$ and $LaCl_3 \cdot 7H_2O$ under the same conditions but the reaction yield was low. No products **2a–2e** were obtained in the presence of $Ni(NO_3)_2 \cdot 6H_2O$, $Zn(NO_3)_2 \cdot 6H_2O$, $ZrCl_4$, or $AgNO_3$ under the same conditions. No explanation can be offered for this outcome. We also performed the coupling reaction of ligands **1b–1e** in the presence of the above mentioned cations under the same conditions giving compounds **2b–2e** (Scheme 1 and Table 1).

Compounds **1a–1e** were synthesized based on the literature procedures⁵ by the reaction of dimedone (**4**) with salicylaldehyde (**5a**), 2-hydroxy-1-naphthaldehyde (**5b**), 2-hydroxy-3-methoxybenzaldehyde (**5c**), 2-hydroxy-5-bromobenzaldehyde (**5d**), and



Scheme 3. Proposed mechanism for the formation of **2a**.

Table 1
Reactions of **1a–1e** with various metal cations

Entry	Metal salt	Yield (%)				
		2a	2b	2c	2d	2e
1	MnCl ₂ ·4H ₂ O	60 ^a	55	75	60	40
2	CuCl ₂ ·2H ₂ O	50	45	60	45	30
3	Cd(NO ₃) ₂ ·4H ₂ O	50	45	60	40	30
4	HgCl ₂	45	40	50	45	35
5	Ni(NO ₃) ₂ ·6H ₂ O	— ^b	—	—	—	—
6	ZrCl ₄	— ^b	—	—	—	—
7	FeCl ₃ ·6H ₂ O	35	30	30	35	30
8	LaCl ₃ ·7H ₂ O	30	25	35	30	30
9	Zn(NO ₃) ₂ ·6H ₂ O	— ^b	—	—	—	—
10	AgNO ₃	— ^b	—	—	—	—

^a Isolated yield.

^b No reaction.

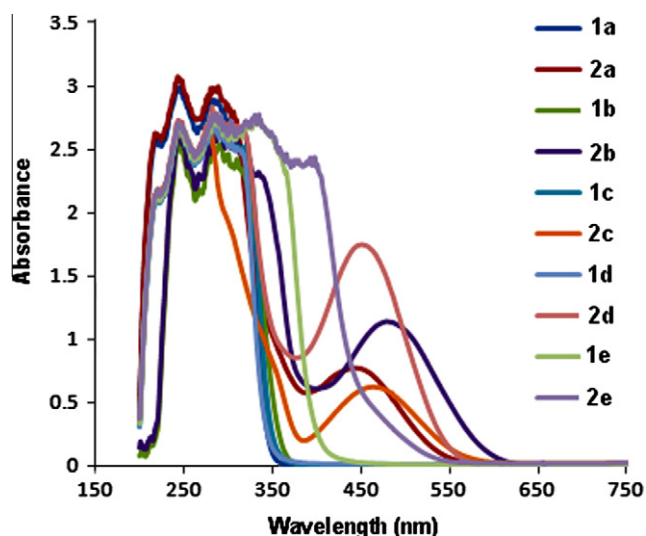


Figure 1. UV-visible spectra of **1a–1e** and **2a–2e** in ethanol.

2-hydroxy-5-nitrobenzaldehyde (**5d**) in acetic acid under reflux (Scheme 2).

The proposed reaction mechanism for the formation of **2a** is shown in Scheme 3. It seems that after formation of complex **3a**, it cleaved to intermediates **6** and **A**. Then the Michael addition of **A** with the β -position of other **A** affords intermediate **B**. This intermediate (**B**) can exist in two mesomeric forms **B[I]** and **B[II]**. The proton capture of these forms affords intermediate **C**. Finally, intermediate **C** converts into **2a** by loss of a proton. In Scheme 3, the nucleophilic attack of fragment **A** was enforced by the lone pair on the oxygen atom. There is some evidence that the bis-dimedone derivative fragmented into two parts on attack of a nucleophilic carbon on a methine carbon.⁶ All attempts to isolate and characterize **6** failed.

The UV-visible spectra of **1a–1e** and corresponding dyes **2a–2e** are shown in Figure 1. The λ_{\max} and corresponding $\log \epsilon_{\max}$ data are summarized in Table 2. The λ_{\max} of ligands **1a–1e** appeared in the ultraviolet absorption region. In contrast, the corresponding products **2a–2e** absorbed in both the ultraviolet and visible regions. Obviously, in dye **2b** the $\pi \rightarrow \pi^*$ (K-band) undergoes a small bathochromic shift due to expansion of the conjugated system involving the naphthyl. In **2e**, this band was hypsochromically shifted due to the electron-withdrawing nitro group on the phenyl rings. The presence of methoxy and bromine substituents on the phenyl rings in **2c** and **2d**, respectively, caused a bathochromic shift with respect to **2a** and **2e** (Fig. 1 and Table 2).

Table 2
UV-visible data of **2a–2e** in ethanol

Compound	λ_{\max}	$\log \epsilon_{\max}$
2a	243, 288, 443	3.074, 2.994, 0.771
2b	244, 285, 488	2.639, 2.642, 1.130
2c	242, 279, 464	2.648, 2.664, 0.617
2d	244, 282, 451	2.730, 2.832, 1.747
2e	244, 284, 335, 398	2.704, 2.769, 2.771, 2.433

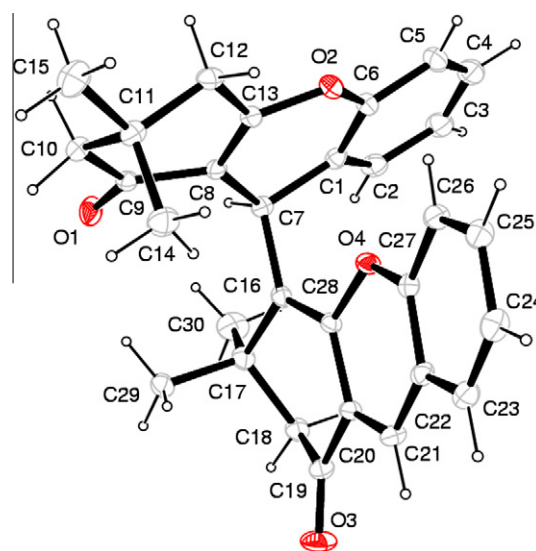


Figure 2. ORTEP drawing of the molecule **2a**. Thermal ellipsoids are shown at 30% probability level.

X-ray diffraction analysis of **2a** was undertaken.⁷ The results of this study confirmed unambiguously the proposed structure (Fig. 2).

Acknowledgment

We thank the Urmia University Research Council for financial support of this work.

Supplementary data

Supplementary data (full characterization of compounds **1a–1e**, **2a–2e** and full crystallographic data of **2a**) associated with this article can be found, in the online version, at <http://dx.doi.org/10.1016/j.tetlet.2012.05.116>.

References and notes

- (a) Gusak, K. N.; Tereshko, A. B.; Kozlov, N. G.; Shakailo, N. I. *Russ. J. Gen. Chem.* **2000**, *70*, 1793–1800; (b) Sato, N.; Jitsuoka, M.; Shibata, T.; Hirohashi, T.; Nonoshita, K.; Moriya, M.; Haga, Y.; Sakuraba, A.; Ando, M.; Ohe, T.; Iwaasa, H.; Gomori, A.; Ishihara, A.; Kanatani, A.; Fukami, T. *J. Med. Chem.* **2008**, *51*, 4765–4770; (c) Sato, N.; Ando, M.; Ishikawa, S.; Jitsuoka, M.; Nagai, K.; Takahashi, H.; Sakuraba, A.; Tsuge, H.; Kitazawa, H.; Iwaasa, H.; Mashiko, S.; Gomori, A.; Moriya, R.; Fujino, N.; Ohe, T.; Ishihara, A.; Kanatani, A.; Fukami, T. *J. Med. Chem.* **2009**, *52*, 3385–3396; (d) Kanatani, A.; Ishihara, A.; Iwaasa, H.; Nakamura, K.; Okamoto, O.; Hidaka, M.; Ito, J.; Fukuroda, T.; MacNeil, D. J.; Van der Ploeg, L. H. T.; Ishii, Y.; Okabe, T.; Fukami, T.; Ihara, M. *Biochem. Biophys. Res. Commun.* **2000**, *272*, 169–173; (e) Morinaka, Y.; Takahashi, K. Jpn. Patent 52017498, 1977 (*Chem. Abstr.* **1977**, *87*, 102299); (f) Witte, E.C.; Neuert, P.; Roesch, A. Ger. Patent DE 3427985, 1986 (*Chem. Abstr.* **1986**, *104*, 224915); (g) Hafez, E. A.; Elnagdi, M. H.; Elagamey, A. A.; El-Taweel, F. A. *Heterocycles* **1987**, *26*, 903–907; (h) Li, Y.-L.; Wang, X.-S.; Shi, D.-Q.; Tu, S.-J.; Zhang, Y. *Acta Cryst.* **2004**, *E60*, o1439–o1441; (i) Lian, C.; Lu, P.; Zhu, Y. *Acta Cryst.* **2009**, *E65*, o2448; (j) Heitz, J. R. *ACS Symp. Ser.* **1995**, *616*, 1–16; (k) Heitz, J. R. In *Insecticide Mode of Action*; Coats, J. R., Ed.; Academic Press: New York, 1982; pp 429–457; (l) Sweet, D.V. *Registry of Toxic Effects of Chemical Substances*, 1986 ed., U.S. Dept. of Health and Human Services, National Institute for Occupational Safety and Health, Cincinnati, Ohio. Pleiades publishing.
- (a) Gordon, P. F.; Gregory, P. In *Critical Reports of Applied Chemistry*; Griffiths, Ed.; Blackwell: Oxford, 1984; Vol 7, pp 81–85; (b) Reinfeld, R.; Brusilovsky, D.; Eyal, M.; Miron, E.; Burstein, Z.; Ivri, J. *Chem. Phys. Lett.* **1989**, *160*, 43–44; (c) Zollinger, H. *Color Chemistry*; New York, Basel-Cambridge: Weinheim, 1991. p 349; (d) Valdes-Aguilera, O.; Neckers, D. C. *Acc. Chem. Res.* **1989**, *22*, 171–177; (e) Valdes-Aguilera, O.; Neckers, D. C. *Adv. Photochem.* **1993**, *18*, 315–394; (f) Chibisov, A. K.; Zakharova, G. V. *Usp. Nauchn. Fotogr.* **1989**, *25*, 114–136; (g) Carmichael, I.; Hug, G. L. *J. Phys. Chem.* **1986**, *15*, 1–250; (h) Marchant, Y. Y. *ACS Symp. Ser.* **1987**, *339*, 168–175; (i) Neckers, D. C. *J. Photochem. Photobiol., A* **1989**, *471*, 1–29; (j) Lopez, A. F.; Lopez, A. T.; Gil, L. E.; Lopez, A. I. *Appl. Fluoresc. Technol.* **1990**, *2*, 8–12; (k) Le, T. H.; Akhtar, M. S.; Park, D. M.; Lee, J. C.; Yang, O-B. *Appl. Catal. B: Environ.* **2012**, *111–112*, 397–401.
- (a) Speiser, S.; Chisena, F. L. *Spec. Publ. Roy. Soc. Chem.* **1989**, *69*, 211–216; (b) Nakayama, N.; Asahina, Y.; Aoki, M.; Fushimi, H.; Makita, K. (to Ricoh Co.), US Patent, 4,933,250 (12, Jun., 1990); (c) Torneiro, M.; Still, W. C. *J. Am. Chem. Soc.* **1995**, *117*, 5887–5888; (d) Hammond, P. R.; Feeman, J. F. U.S. Patent, 5,111,472 (May 5, 1992).
- General procedure. Preparation of 3,3,3',3'-tetramethyl-2,3,3',4'-tetrahydro-1H,1'H-[4,9'-bixanthene]-1,1'-(2'H,9'H)-dione (2a).** In a 25 mL round bottomed flask a mixture of **1a** (0.10 g, 0.27 mmol) and MnCl₂·4H₂O (0.05 g, 0.27 mmol) was dissolved in EtOH (10 mL) and was refluxed for 96 h. After a few minutes the solution became orange then red. The reaction progress was monitored by thin layer chromatography (TLC) using a mixture of EtOAc: n-hexane (2:1 v:v) as solvent. The crude red reaction mixture was purified by preparative thin-layer chromatography (silica gel type 60F254). After separation, the solution was dried over MgSO₄ and filtered. Finally, an orange crystalline solid was obtained (0.075 g, 60%). A single crystal of **2a** was obtained by slow evaporation from EtOH at room temperature. Orange crystalline solid; mp 184–185 °C; FT-IR (KBr): 3049, 2955, 2930, 1637, 1582, 1389, 1236, 1179, 766 cm⁻¹; ¹H NMR (CDCl₃, 300 MHz) δ 7.20 (t, 2H, J = 6.6 Hz), 7.05–7.10 (m, 3H), 6.94–6.98 (m, 3H), 6.87 (t, 1H, J = 6.6 Hz), 4.85 (s, 1H), 2.29–2.64 (m, 6H), 1.48 (s, 6H), 1.11 (s, 3H), 0.95 (s, 3H); ¹³C NMR (CDCl₃, 75 MHz) δ 197.2, 197.0, 165.9, 155.3, 150.5, 146.3, 131.9, 129.5, 129.0, 127.4, 124.7, 124.5, 124.3, 122.7, 119.9, 115.9, 114.7, 111.2, 76.6, 54.9, 53.4, 51.2, 42.2, 35.5, 32.0, 29.5, 29.3, 27.9, 27.8, 26.9; Elemental analysis calcd (%) for C₃₀H₂₈O₄ (452.55): C 79.54, H 6.19; found (%): C 79.56, H 6.56; UV data (EtOH): λ_{max} (log ε_{max}) = 243, 288, 443 nm, (3.074, 2.994, 0.771).
- (a) Wang, X.-S.; Shi, D.-Q.; Li, Y.-L.; Chen, H.; Wei, X.-Y.; Zong, Z.-M. *Synth. Commun.* **2005**, *35*, 97–104; (b) Zhang, P.; Yu, Y.-D.; Zhang, Z.-H. *Synth. Commun.* **2008**, *38*, 4474–4479.
- Gheath, A. H.; Al-Orffi, N. M. *Science and Its Applications* (Garyounis University Press) 2008, *2*, 60–68.
- For the crystal structure determination, a single-crystal of compound **2a** was used for data collection on a four-circle Rigaku R-AXIS RAPID-S diffractometer (equipped with a two-dimensional area IP detector). Graphite-monochromated MoKα radiation (λ = 0.71073 Å) and oscillation scans technique with Δω = 5 for one image were used for data collection. The lattice parameters were determined by the least-squares methods on the basis of all reflections with F² > 2σ(F²). Integration of the intensities, correction for Lorentz and polarization effects and cell refinement was performed using CrystalClear (Rigaku/MSC Inc., 2005) software.⁸ The structures were solved by direct methods using SHELXS-97⁹ and refined by a full-matrix least-squares procedure using the program SHELXL-97.⁹ H atoms were positioned geometrically and refined using a riding model. The final difference Fourier maps showed no peaks of chemical significance. Crystal data for **2a**: C₃₀H₂₈O₄, crystal system, space group: triclinic, P-1; (no:2); unit cell dimensions: a = 9.4434(2), b = 10.0078(2), c = 14.2287(4) Å, α = 70.47(3), β = 85.76(2), γ = 70.1983(3)°; volume: 1191.2(2) Å³; Z = 2; calculated density: 1.262 g/cm³; absorption coefficient: 0.083 mm⁻¹; F(000): 480; θ-range for data collection 2.3–26.5°; refinement method: full-matrix least-square on F²; data/parameters: 4882/311; goodness-of-fit on F²: 1.012; final R-indices [I > 2σ(I)]: R₁ = 0.079, wR₂ = 0.191; R-indices (all data): R₁ = 0.189, wR₂ = 0.283; largest diff. peak and hole: 0.205 and -0.224 e Å⁻³; Crystallographic data that were deposited in CSD under CCDC registration number 848935 contain the supplementary crystallographic data for this Letter. These data can be obtained free of charge from the Cambridge Crystallographic Data Centre (CCDC) via www.ccdc.cam.ac.uk/data_request/cif and are available free of charge upon request to CCDC, 12 Union Road, Cambridge, UK (fax: +44 1223 336033, e-mail: deposit@ccdc.cam.ac.uk).
- Rigaku/MSC, Inc.: 9009 new Trails Drive, The Woodlands, TX 77381.
- Sheldrick, G. M. *SHELXS97* and *SHELXL97*; University of Göttingen: Germany, 1997.